0026-895X/91/030413-08$03.00/0

MOLECULAR PHARMACOLOGY, 40:413-420

Binding Kinetics of Quinuclidinyl Benzilate and Methyl-quinuclidinyl Benzilate Enantiomers at Neuronal (M_1), Cardiac (M_2), and Pancreatic (M_3) Muscarinic Receptors

MAGALI WAELBROECK, MICHELE TASTENOY, JEAN CAMUS, and JEAN CHRISTOPHE
Department of Biochemistry and Nutrition, Medical School, Université Libre de Bruxelles, B-1000 Brussels, Belgium
Received March 4, 1991; Accepted June 3, 1991

SUMMARY

We analyzed the competition kinetics of quinuclidinyl benzilate (QNB) and QNB methiodide enantiomers on human NB-OK1 neuroblastoma (M_1), rat cardiac (M_2), and rat pancreas (M_3) muscarinic binding sites. The association rate constants of the four drugs depended on the receptor subtype studied and were lower with pancreas (M_3) ($1-9 \times 10^5$ M^{-1} sec^{-1}) than with cardiac (M_2) ($1-5 \times 10^6$ M^{-1} sec^{-1}) and NB-OK1 (M_1) ($1-5 \times 10^6$ M^{-1} sec^{-1}) binding sites. At each receptor subtype, we observed no significant difference between the association rate constants of the *R*- and *S*-enantiomers of either QNB or QNB methiodide. Receptor stereoselectivity, when present, was associated with differences in unlabeled drug dissociation rate constants. The dissociation rate constant varied much more than the association rate constant, when either (*R*)-QNB dissociation from the three subtypes (half-life, 77 min to >340 min; best fit, 40 days) or dissociation of the four drugs from each receptor subtype (half-lives varying from 1.4 min to 4 hr at M_1 receptors, 1.1 to 77 min at M_2 receptors, and 3.5 min to >340 min at M_3 receptors were obtained by competition kinetics analysis) was compared.

The presence of at least three subtypes of muscarinic receptors in mammalian tissues is now well established (1). Human NB-OK1 neuroblastoma cell receptors show typical M_1 selectivity in binding studies, including high affinity for pirenzepine (2). Rat heart receptors manifest M_2 selectivity, i.e., low affinity for pirenzepine but high affinity for AF-DX 116 (3). Rat pancreas receptors display M_3 selectivity, i.e., low affinity for pirenzepine and AF-DX 116 and high affinity for 4-DAMP and hexahydro-sila-difenidol (3). To the binding properties and tissue distribution of these receptors correspond, respectively, the recently cloned m1, m2, and m3 RNAs (1). A fourth subtype was recently identified in rat striatum (4) and guinea pig uterus (5) and might correspond to the m4 mRNA.

We have already demonstrated that M_1, M_2, and M_3 muscarinic receptor subtypes can be discriminated otherwise than by highly selective antagonists. Indeed, 1) the dissociation rate constant of the nonselective antagonist [^{3}H]NMS also varies among muscarinic receptor subtypes (6), and 2) the capacity of M_1, M_2, and M_3 receptors to recognize the enantiomers of chiral drugs is often different (7).

This work was supported by Grant 3.4571.85 from the Fund for Medical Scientific Research (Belgium).

It is possible to determine the association and dissociation rate constants of an unlabeled drug by measuring the binding kinetics of a tracer in the absence and presence of this drug (8). If the unlabeled drug binds faster than the tracer to the receptors, it will effectively prevent tracer binding at short incubations. The tracer dissociation kinetics will, therefore, appear slower in the presence than in the absence of the unlabeled drug. If, in contrast, the unlabeled drug binds more slowly than the tracer, inhibition of tracer binding will develop progressively with time (8).

We previously analyzed the binding kinetics of seven muscarinic antagonists in rat pancreas, using this "competition kinetics" approach (9). To our surprise, the value of the association rate constants of muscarinic antagonists varied by >2 orders of magnitude, depending on the drug studied. This result suggested that the muscarinic antagonist-receptor binding reaction is controlled by a rate-limiting step that depends on the drug structure.

To investigate the importance of the absolute drug configuration (stereochemistry) for this rate-limiting step, we decided to compare the binding properties of pairs of enantiomers interacting with muscarinic receptors. We observed recently that muscarinic receptors show, in binding studies, a poor

ABBREVIATIONS: AF-DX 116, 11-{[2-[(diethylamino)methyl]-1-piperidinyl]acetyl}-5,11-dihydro-6*H*-pyrido(2,3-*b*)(1,4)benzodiazepine-6-one; [^{3}H]NMS, 1-[*N-methyl*-^{3}H]scopolamine methyl chloride; 4-DAMP, 4-diphenylacetoxy-*N*-methylpiperidine methiodide; QNB, quinuclidinyl benzilate; methyl-QNB or QNB$^+$, *N*-methyl QNB iodide; K_D and K_i, equilibrium dissociation constant of the tracer or unlabeled drug, respectively; k_{on} and k_{off}, association and dissociation rate constants, respectively; of the tracer; k_3 and k_4, association and dissociation rate constants, respectively, of the unlabeled drug.

stereoselectivity for the enantiomers of QNB and methyl-QNB (7). Others have also shown that these compounds recognize muscarinic receptors quite slowly (10–14). We, therefore, thought that these compounds were good candidates for measurement of the association and dissociation rate constants of two enantiomers at several receptors; indeed, if an unlabeled drug equilibrates too quickly with muscarinic receptors, it is not possible to obtain meaningful estimates of the rate constants.

We took advantage of the fact that human neuroblastoma NB-OK1 cells, rat heart, and rat pancreas contain, respectively, 80% M_1, 100% M_2, and 100% M_3 muscarinic receptors (2, 3) to investigate the binding kinetics of each compound at three muscarinic receptor subtypes. We used (*R*)-[^{3}H]QNB and (*R*)-[^{3}H]QNB methyl chloride to measure directly the dissociation rate constants of these (high affinity) enantiomers in NB-OK1 cells and heart homogenates and validate the constants obtained by competition kinetic analyses. The dissociation rate constants of (*R*)-methyl-QNB obtained by the two methods were in excellent agreement; the dissociation rate constants of (*R*)-[^{3}H]QNB (direct measurement) were not significantly slower than those of (*R*)-QNB (competition kinetics), in both tissues.

Our results indicate that 1) the M_1, M_2, and M_3 muscarinic receptor stereoselectivity is associated with major differences in drug-receptor complex dissociation rate constants and 2) the "nonselective" QNB and methyl-QNB *R*- and *S*-enantiomers dissociate at different rates from the three muscarinic receptor subtypes.

Experimental Procedures

Chemicals. [^{3}H]NMS (specific radioactivity, 85 Ci/mmol) and (*R*)-[^{3}H]QNB (specific radioactivity, 42 Ci/mmol) were obtained from Amersham International (Bucks, UK). (*R*)-[^{3}H]QNB methyl chloride (specific radioactivity, 87 Ci/mmol) was obtained from New England Nuclear (Boston, MA). Atropine and polyethyleneimine were purchased from Sigma Chemical Co. (St. Louis, MO). QNB and methyl-QNB enantiomers of very high optical purity (13, 14) were generous gifts from Dr. G. Lambrecht (Department of Pharmacology, University of Frankfurt/M, FRG) (9, 10).

Methods. The NB-OK1 cell line was cultured and cell homogenates were prepared as described (2). Heart and pancreas homogenates were obtained as described (3).

For competition kinetic studies, the homogenates were incubated, at 25°, with [^{3}H]NMS and the unlabeled drug for 5 min, 10 min, 20 min, 1 hr, 2 hr, and 4 hr, in 1.2 ml of 50 mM sodium phosphate buffer (pH 7.4) enriched with 2 mM $MgCl_2$, 1% bovine serum albumin, and, in addition, in the case of pancreas homogenates, 0.2 mg/ml bacitracin and 500 kallikrein inhibiting units of aprotinin (Trasylol Bayer). Tracer binding was measured by a filtration method, as previously described (2, 3).

To measure the dissociation rate of (*R*)-[^{3}H]QNB and (*R*)-[^{3}H]QNB methyl chloride from NB-OK1 and cardiac receptors, the homogenates were preincubated in the same buffer at 25° with 1 nM tracer, for 15 min or 2 h. We then added atropine or *N*-methyl-atropine (1 μM) to each sample to induce tracer dissociation and measured residual tracer binding (by filtration) as a function of time. To measure (*R*)-[^{3}H]QNB and (*R*)-[^{3}H]QNB methyl chloride dissociation from pancreas receptors, the homogenates were preincubated for 4 hr at 25° either in a total volume of 1.2 ml [with 0.2 nM (*R*)-[^{3}H]QNB or 0.1 nM (*R*)-[^{3}H]QNB methyl chloride and 1 mg/assay pancreas protein] or in a total volume of 5.0 ml [with 0.05 nM (*R*)-[^{3}H]QNB or 0.025 nM (*R*)-[^{3}H]QNB methyl chloride and 2 mg/assay pancreas protein], in the absence or presence of dexetimide (0.1 nM to 10.0 μM), in quadruplicate. After this preincubation, duplicate tubes were filtered to measure tracer binding to genuine muscarinic receptors. Atropine was added to the remaining duplicates, to achieve a final concentration of 1 μM. The incubation was then continued for 1 hr [with (*R*)-[^{3}H]QNB methyl chloride] or 4 hr [with (*R*)-[^{3}H]QNB], before filtration. The competition curves were analyzed by a nonlinear regression curve-fitting procedure.

To analyze quantitatively the binding kinetics of both enantiomers to the three receptor subtypes, we used the equations developed by Motulsky and Mahan (8), as described previously (9). We initially calculated the apparent K_i value of the unlabeled drug, using the competition curves obtained after a 4-hr incubation. We then attempted to fit the nonequilibrium competition curves (5-min to 2-hr incubation) by varying k_3 and k_4 values stepwise while holding their ratio $K_i = k_4/k_3$ constant. We searched the values of k_3 and k_4 corresponding to the lowest sum of squared differences between experimental and fitted values. In a second step, we allowed variations of the $K_i = k_4/k_3$ value, holding alternatively k_3 or k_4 constant, and attempted to obtain an even lower sum of squared differences. In one case [(*R*)-QNB binding to M_3 receptors], we were unable to obtain a single best fit estimate of k_4 and K_i; the reaction was so slow that the fitted curves were independent of the actual value of k_4 or K_i (as long as $k_4 \leq 2 \times 10^{-7}$ sec^{-1}). As shown in Figs. 1 to 4, where symbols correspond to experimental data points and lines to fitted curves, we were able to achieve a very good fit of experimental data in the three systems tested.

To estimate 95% confidence intervals, we compared the expected and experimental data either at a single drug concentration (and six incubation periods) or at a single incubation period (and seven drug concentrations), assuming different k_3 and k_4 values. We used a *F* test to determine the values of k_3 and k_4 giving such a bad fit of experimental data that the probability of obtaining our experimental results with a drug having those k_3 and k_4 values is below 5% ($p < 0.05$).

Results

M_1 receptors in NB-OK1 cell homogenates. As shown in Fig. 1 (*lower*) (*R*)-QNB competition curves obtained after 4 hr of incubation at 25° were very steep ($n_H = 1.4$). We were worried about (*R*)-QNB depletion by muscarinic receptors, because the receptor concentration (20–40 pM, as estimated from [^{3}H]NMS saturation curves; data not shown) was close to the (*R*)-QNB K_i value (below 50 pM). This was apparently not significant in our case, because 1) the Hill coefficient ($n_H = 1.3$) was just as high when a very high tracer concentration (1.6 nM) was used to inhibit (*R*)-QNB binding (Fig. 2) and 2) the concentration of (*R*)-QNB necessary to inhibit 50% of tracer binding was increased when the tracer concentration rose from 0.24 nM to 1.6 nM, as expected from competitive binding between [^{3}H]NMS and (*R*)-QNB (apparent K_i = 50 pM) (Fig. 2). To remain on the safe side, however, we performed the (*R*)-QNB competition kinetics (Fig. 2) using a high (1.6 nM) [^{3}H]NMS concentration.

The comparison of (*R*)-QNB competition curves, obtained after various incubation periods (Fig. 2), suggested that this antagonist bound very slowly to muscarinic receptors; competition curves shifted to the lower concentration range with increasing incubation time. They could be fitted using the Motulsky and Mahan equations (8), assuming that (*R*)-QNB had a K_i of 32 pM and a dissociation half-life of 220 min (almost 4 hr). The best fit parameters are given in Tables 2 and 3. The Motulsky and Mahan model (8) predicts "steep" competition curves after short incubation periods, due to faster binding at high drug concentrations. In other words, unlabeled drug binding is more severely underestimated at low than at high drug concentrations, when the incubation period is too short (i.e., 4

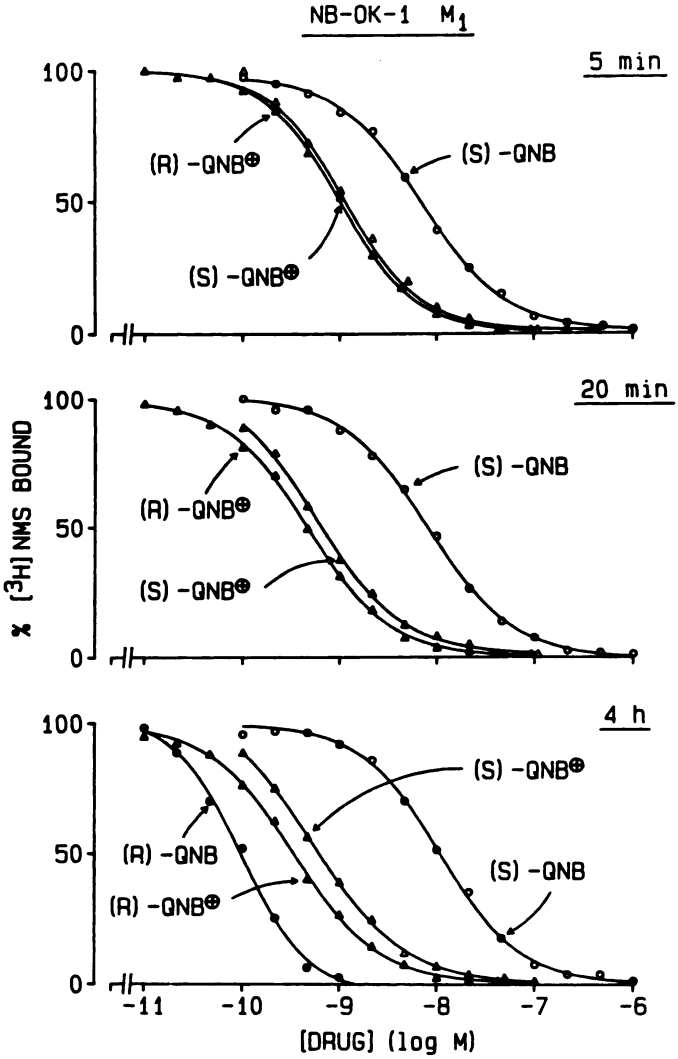

Fig. 1. Competition curves of QNB and methyl-QNB enantiomers in NB-OK1 cell homogenates. [^{3}H]NMS (0.24 nM) binding was measured as a function of time, in the absence or presence of (*R*)-QNB (●) (4 hr only), (*R*)-methyl-QNB (▲), (*S*)-QNB (○), or (*S*)-methyl-QNB (△). The incubation periods were 5 min (*top*), 20 min (*center*) or 4 h (*bottom*). The (*R*)-QNB competition kinetics are shown in Fig. 2. The best fit parameters used for curve fitting, and their 95% confidence intervals, are shown in Table 2. Average of three experiments performed in duplicate. The standard deviation was always <5% of control binding (100%).

hr or shorter in the present case).

(*S*)-QNB, (*R*)-methyl-QNB, and (*S*)-methyl-QNB competition curves gave a Hill coefficient of 1.0 after a 4-hr incubation (Fig. 1). The (*S*)-QNB competition curve was slightly shifted to the higher concentration range by increasing of the incubation period from 5 min to 4 hr. This result indicates that (*S*)-QNB equilibrated faster than [^{3}H]NMS with these muscarinic receptors and that the tracer progressively displaced the unlabeled drug after longer incubations (Tables 1 and 2). The (*R*)-methyl-QNB and (*S*)-methyl-QNB competition curves were very slightly shifted to the lower concentration range by increasing of the incubation period from 5 min to 4 hr, suggesting that their dissociation rate constants from M_1 muscarinic receptors were comparable to or slightly lower than the [^{3}H]NMS dissociation rate constant (Tables 1 and 2).

M_2 receptors in rat heart homogenates. The Hill coefficients of the four competition curves obtained after 4 hr of

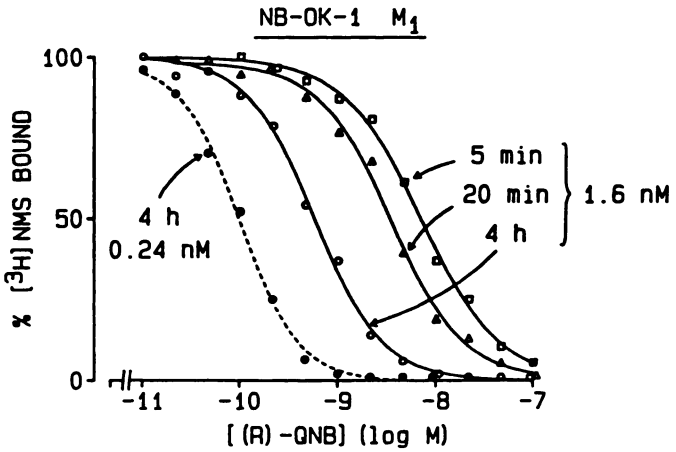

Fig. 2. (*R*)-QNB competition curves in NB-OK1 cell homogenates. (*R*)-QNB competition curves were obtained in the presence of 0.24 nM [^{3}H]NMS after 4 hr of incubation (●) or 1.6 nM [^{3}H]NMS (*open symbols*) after 5 min (□), 20 min (△), or 4 h (○) of incubation. The best fit parameters used for curve fitting, and their 95% confidence intervals, are shown in Table 2. Average of three experiments performed in duplicate. The standard deviation was always <5% of control binding (100%).

TABLE 1

Association (k_{on}) and dissociation (k_{off}) rate constants and equilibrium dissociation constants (K_D) of [^{3}H]NMS binding to human NB-OK1 neuroblastoma (M_1), rat heart (M_2), and rat pancreas (M_3) homogenates

These values, published in Refs. 2, 3, and 9, allowed us to interpret the experimental data in Figs. 1–5 and to calculate the data in Tables 2 and 3.

Homogenate	k_{on}	k_{off}	K_D
	M^{-1} sec^{-1}	sec^{-1}	nM
NB-OK1 (M_1)	1.40×10^7	1.7×10^{-3}	0.12
Heart (M_2)	1.17×10^7	5.8×10^{-3}	0.40
Pancreas (M_3)	2.00×10^6	2.0×10^{-4}	0.10

incubation were equal to 1.1 for (*R*)-QNB and to 1.0 for (*S*)-QNB, (*R*)-methyl-QNB, and (*S*)-methyl-QNB (Fig. 3). The concentration of muscarinic receptors in the assay (40–60 pM, as estimated by [^{3}H]NMS Scatchard plots; data not shown) was lower than the unlabeled drug concentration necessary for 50% [^{3}H]NMS binding inhibition. On this basis, we decided to perform kinetic experiments at a low 1 nM tracer concentration, equivalent to 2.5 × the K_D value in this system (Table 1). Under these conditions, competition curves reflected unlabeled drug binding with little contribution from competition by [^{3}H]NMS.

(*R*)-QNB competition curves were shifted towards the lower concentration range with increasing incubation times and were steep after short incubations (n_H = 1.30 after 5 min and 1.35 after 20 min). This indicated that (*R*)-QNB equilibrated slowly with cardiac muscarinic receptors. (*S*)-QNB and (*S*)-methyl-QNB competition curves did not vary with the incubation period, indicating that these enantiomers equilibrated with cardiac receptors at a rate comparable to that of [^{3}H]NMS. (*R*)-Methyl-QNB competition curves were steep (n_H = 1.3) after a 5-min incubation and slightly shifted to the lower concentration range by prolonged incubations; this drug bound more slowly than [^{3}H]NMS to M_2 receptors. Short (20-min) incubations sufficed, however, to reach equilibrium binding. The kinetic constants are shown in Tables 2 and 3.

M_3 receptors in rat pancreas homogenates. [^{3}H]NMS binds very slowly to pancreas receptors (3). We, therefore, decided to use a high tracer concentration in order to obtain

TABLE 2

Association (k_3) and dissociation (k_4) rate constants and equilibrium dissociation constants (K_i) of (*R*)- and (*S*)-QNB and methyl-QNB enantiomers, in NB-OK1 cell (80% M_1 sites), rat heart (100% M_2 sites), and rat pancreas (100% M_3 sites) homogenates

These values were estimated by analysis of [^{3}H]NMS competition curves after six incubation periods or at seven unlabeled drug concentrations. The 95% confidence intervals of the kinetic constants (see Experimental Procedures) are indicated in parentheses under each best fit value.

Homogenate	Drug	k_3	k_4	K_i
		$M^{-1} \cdot sec^{-1}$	sec^{-1}	nM
NB-OK1 (M_1)	(*R*)-QNB	1.6×10^6 (9×10^5–2×10^6)	5.3×10^{-5} (3×10^{-5}–7.0×10^{-5})	0.032
	(*S*)-QNB	2.4×10^6 (9.4×10^5–large)	8.3×10^{-3} (3.3×10^{-3}–large)	3.5
	(*R*)-QNB$^+$	5.4×10^6 (3.8×10^6–8.5×10^6)	7.0×10^{-4} (5.0×10^{-4}–1.1×10^{-3})	0.13
	(*S*)-QNB$^+$	5.3×10^6 (4.2×10^6–9.2×10^6)	1.27×10^{-3} (1.0×10^{-3}–2.2×10^{-3})	0.24
Heart (M_2)	(*R*)-QNB	1.7×10^6 (1.1×10^6–3.7×10^6)	1.5×10^{-4} (1.0×10^{-4}–3.3×10^{-4})	0.09
	(*S*)-QNB	1.85×10^6 (2.9×10^5–large)	1.0×10^{-2} (1.6×10^{-3}–large)	5.4
	(*R*)-QNB$^+$	4.3×10^6 (2.6×10^6–1.2×10^7)	1.8×10^{-3} (1.1×10^{-3}–5×10^{-3})	0.43
	(*S*)-QNB$^+$	9.7×10^6 (3.0×10^6–large)	4.2×10^{-3} (1.3×10^{-3}–large)	0.43
Pancreas (M_3)	(*R*)-QNB	1.8×10^5	See text (0–3.4×10^{-5})	(<0.2)
	(*S*)-QNB	1.6×10^5 (1.3×10^5–3.6×10^5)	1.8×10^{-3} (1.4×10^{-3}–4.0×10^{-3})	11.0
	(*R*)-QNB$^+$	3.9×10^5 (2.3×10^5–1.2×10^6)	2.5×10^{-4} (1.6×10^{-4}–7.5×10^{-4})	0.65
	(*S*)-QNB$^+$	8.3×10^5 (3.2×10^5–large)	3.3×10^{-3} (1.3×10^{-3}–large)	4.0

sufficient tracer binding after short incubation periods. The Hill coefficients of the four competition curves (shown in Fig. 4) were slightly greater than 1 after short incubation periods (1.1–1.2 after a 5-min incubation) and, with time, decreased progressively towards unity [except for (*R*)-QNB, $n_H = 1.15$ after 4 hr of incubation].

The (*R*)-QNB competition curve shifted markedly towards the lower concentration range with increasing incubation periods, despite enhanced competition by the large [^{3}H]NMS concentration. Our results indicated that (*R*)-QNB dissociation from M_3 receptors was very slow; we measured (indirectly) the initial binding of (*R*)-QNB. The association rate constant at M_3 receptors (1.8×10^5 M^{-1} sec^{-1}) was very low, compared with M_1 or M_2 receptors, but similar to that of (*S*)-QNB and (*R*)- and (*S*)-methyl-QNB binding to M_3 receptors (see below; Table 2). The dissociation rate constant k_4 could not be measured with precision, with the 95% confidence interval ranging from 0 to 3.4 10^{-5} sec^{-1}. As a result, the K_i value of (*R*)-QNB for pancreas M_3 receptors could not be measured (95% confidence interval, 0–200 pM).

The best fit competition kinetics shown in Fig. 4 were calculated assuming that the dissociation rate constant of (*R*)-QNB was equal to or less than 2×10^{-7} sec^{-1} ($K_i = k_4/k_3 \leq 1$ pM). According to this hypothesis, (*R*)-QNB would have a strong selectivity for M_3 receptors at equilibrium, with an incubation period of almost 2.5 months (1.75 half-life) (8) being necessary to approach equilibrium at the IC_{50} concentration. (*S*)-QNB and (*S*)-methyl-QNB equilibrated rapidly with pancreas muscarinic receptors; [^{3}H]NMS progressively displaced the unlabeled drug bound to M_3 receptors and shifted the competition curve to the higher concentration range. (*R*)-Methyl-QNB competition curves shifted only slightly towards the lower concentration range with increasing incubation times, suggesting that its dissociation rate constant was close to that of [^{3}H]NMS. The best fit kinetic constants are shown in Tables 2 and 3.

Comparison of the binding properties of labeled and unlabeled (*R*)-QNB and (*R*)-QNB methiodide (methyl chloride) at the three muscarinic receptor subtypes. We investigated the binding properties of the labeled, "active" *R*-enantiomers of QNB and methyl-QNB in the three cell and tissue preparations (results not shown).

In NB-OK1 cell homogenates, (*R*)-[^{3}H]QNB labeled M_1 muscarinic receptors, of which 85% were accessible and 15% inaccessible to quaternary ligands (including NMS). Its saturation curve was monophasic. We observed an identical dissociation rate ($k_{off} = 2.0 \pm 0.5 \times 10^{-5}$ sec^{-1}; $t_{1/2} = 10$ hr) after addition of either atropine or *N*-methylatropine (to prevent tracer binding either to all binding sites or to the 85% NMS binding sites only). The dissociation rate of (*R*)-[^{3}H]QNB was constant for at least 6 hr (allowing 35% dissociation) and did not change when the preincubation period was increased from 15 min to 2 hr. (*R*)-[^{3}H]Methyl-QNB labeled the same receptor population as [^{3}H]NMS in NB-OK1 cell homogenates. Its saturation curve was monophasic. The dissociation of (*R*)-[^{3}H]methyl-QNB from NB-OK1 receptors was monoexponential, with a k_{off} value of $7.2 \pm 1.5 \times 10^{-4}$ sec^{-1} ($t_{1/2}$ of 16 min). This result suggested that the dissociation rate constants of (*R*)-[^{3}H]methyl-QNB for M_1 receptors (80%) and M_3/M_4 receptors (20%) differed by 10-fold or less (see Table 2 for a comparison of k_4 of (*R*)-methyl-QNB from M_1 and M_3 sites).

In cardiac homogenates, (*R*)-[^{3}H]QNB and (*R*)-[^{3}H]methyl-QNB recognized the same receptor population as [^{3}H]NMS. The dissociation of both tracers was monoexponential. (*R*)-[^{3}H]QNB had a dissociation rate constant of $7.7 \pm 1.6 \times 10^{-5}$ sec^{-1} ($t_{1/2} = 2.5$ hr) and (*R*)-[^{3}H]methyl-QNB of $1.9 \pm 0.4 \times$

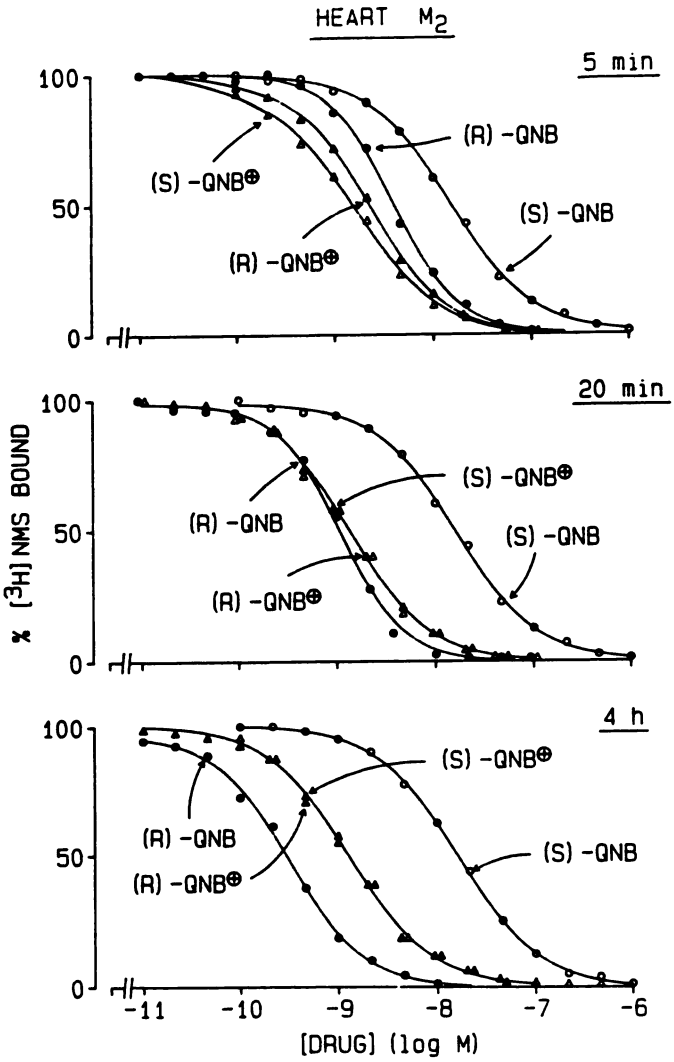

Fig. 3. Competition curves of QNB and methyl-QNB enantiomers in rat heart homogenates. The [^{3}H]NMS concentration was 1.0 nM, and the incubation periods were 5 min (*top*), 20 min (*center*), or 4 h (*bottom*). The best fit parameters used for curve fitting, and their 95% confidence intervals, are shown in Table 2. Average of three experiments performed in duplicate. The standard deviation was always <5% of control binding (100%).

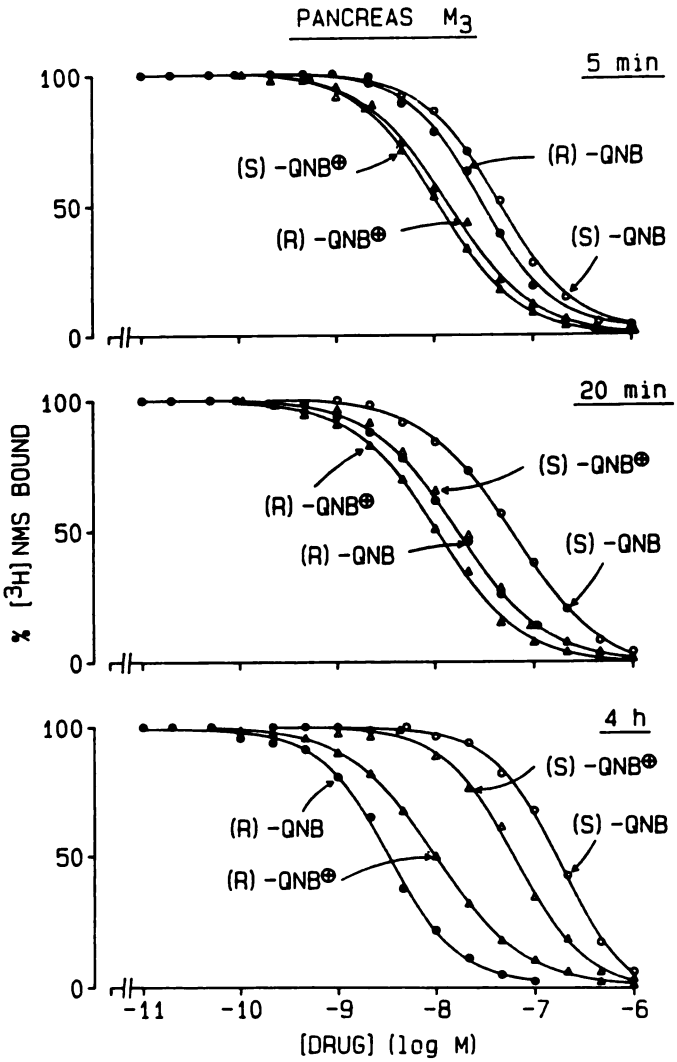

Fig. 4. Competition curves of QNB and methyl-QNB enantiomers in rat pancreas homogenates. The [^{3}H]NMS concentration was 1.6 nM, and the incubation periods were 5 min (*top*), 20 min (*center*), or 4 hr (*bottom*). The best fit parameters used for curve fitting, and their 95% confidence intervals, are summarized in Table 2, except those for (*R*)-QNB. The latter competition kinetics were fitted assuming that $k_3 = 1.8 \times 10^5$ M^{-1} sec^{-1}, $k_4 = 2 \times 10^{-7}$ sec^{-1} (confidence interval, 0–3.4×10^{-5} sec^{-1}), and K_i = 1 pM (confidence interval, 0–200 pM) (see text). Average of three experiments performed in duplicate. The standard deviation was always <5% of control binding (100%).

TABLE 3

Half-life of drug-muscarinic receptor complexes derived from dissociation rate constants (k_4) (see Table 2)

Drug	Half-life		
	M_1	M_2	M_3
		min	
(*R*)-QNB	220	77	>340[a]
(*S*)-QNB	1.4	1.1	4.6
(*R*)-QNB$^+$	17	6.4	46
(*S*)-QNB$^+$	9	2.8	3.5

[a] Our experimental values would be obtained in only 5% of repeated experiments if the half-life of the (*R*)-QNB-M_3 receptor complex was as short as 340 min. The actual best fit value used to fit Fig. 4 was 40 days.

10^{-3} sec^{-1} ($t_{1/2}$ = 10 min).

In pancreas homogenates, (*R*)-[^{3}H]QNB and (*R*)-[^{3}H]methyl-QNB recognized two binding sites. The first binding site displayed the characteristics of a true muscarinic receptor, i.e., high affinity for (*R*)-[^{3}H]QNB, (*R*)-[^{3}H]methyl-QNB, and [^{3}H]NMS, high affinity for atropine (EC_{50} = 1–2 nM) and dexetimide (EC_{50} = 0.5–1.0 nM), and very low affinity for levetimide (EC_{50} = 50–100 μM). The second binding site was not labeled by [^{3}H]NMS, had a very low affinity for (*R*)-[^{3}H]QNB and (*R*)-[^{3}H]methyl-QNB, and had a low affinity for atropine (EC_{50} ~ 250 nM) and levetimide (EC_{50} ~ 750 nM). Binding to this second site represented 50–60% of total (*R*)-[^{3}H]QNB and (*R*)-[^{3}H]methyl-QNB binding under our usual assay conditions (1.2 ml, 0.1–0.2 nM tracer concentration) but could be decreased to 25–35% of total tracer binding by decreasing the tracer concentration while increasing the incubation volume (see Experimental Procedures). We, therefore, used a dexetimide competition curve to evaluate (*R*)-[^{3}H]QNB and (*R*)-[^{3}H]methyl-QNB binding to genuine muscarinic receptors. To measure the dissociation of these tracers from pancreas (M_3) muscarinic receptors, we preincubated the homogenates

in the presence of tracer and in the absence or presence of dexetimide (0.1 nM to 10 μM). After a 4-hr preincubation, one set of samples was filtered to measure initial binding, and atropine (1 μM) was added to a second set to induce tracer dissociation. The latter samples were filtered either 1 hr [for (*R*)-[^{3}H]methyl-QNB] or 4 hr [for (*R*)-[^{3}H]QNB] after atropine addition. The dexetimide competition curves were analyzed with a nonlinear curve-fitting program to determine tracer binding to "muscarinic sites" showing high affinity for dexetimide. We were unable to detect any (*R*)-[^{3}H]QNB dissociation 4 hr after atropine addition to pancreas homogenates; residual tracer binding to muscarinic sites amounted to 105 ± 15% of initial binding. In contrast, the residual (*R*)-[^{3}H]methyl-QNB binding to muscarinic receptors, 1 hr after atropine addition, corresponded to only 37 ± 10% of initial binding. Assuming monoexponential tracer dissociation, this corresponded to a k_{off} value of 2.8×10^{-4} sec^{-1} ($t_{1/2}$ = 42 min).

Effect of time on the calculated apparent affinity (K_i) of QNB and QNB methiodide enantiomers. We calculated the concentration of QNB and methyl-QNB enantiomers that was necessary to occupy 50% of muscarinic binding sites (in the absence of tracer), considering that the incubation period varied from 5 min to 4 hr and using the rate constants found by competition kinetic analysis. The results (plotted on a logarithmic scale) are shown in Fig. 5.

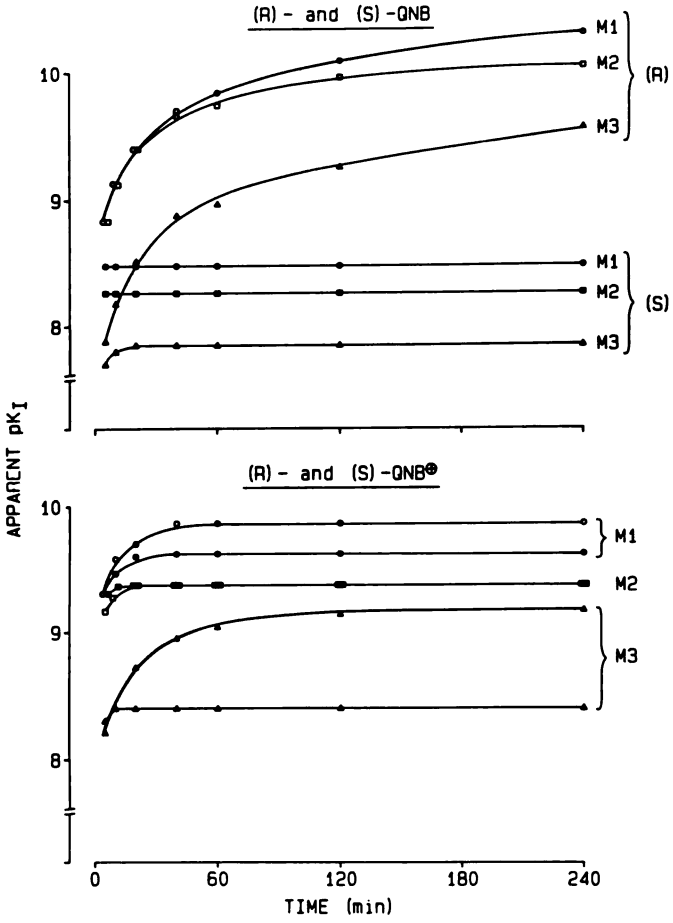

Fig. 5. Calculation of the concentration of QNB and methyl-QNB enantiomers necessary to occupy 50% of receptors (apparent K_i), as a function of time, using rate constants in Table 2. The results were plotted on a logarithmic scale ($pK_i = -\log K_i$).

(*R*)-QNB reached equilibrium very slowly; a 4-hr incubation was barely sufficient to allow equilibrium binding at M_2 receptors (and too short for M_1 and M_3 receptors). (*R*)-Methyl-QNB apparent affinity increased less slowly with time and reached equilibrium after 20 min at M_2 sites, 1 hr at M_1 sites, and 4 hr at M_3 sites. The *S*-enantiomers of QNB and methyl-QNB reached equilibrium within 20 min at the three muscarinic receptor subtypes.

From these kinetic differences, it resulted that the muscarinic receptor stereoselectivity for QNB and methyl-QNB enantiomers was scarcely detectable after a short (5-min) incubation and increased progressively with time.

Discussion

We have previously demonstrated that, in rat pancreas homogenates, the affinity of several antagonists for muscarinic receptors is not correlated with their dissociation rate constant and that their association rate constant is highly variable (9). We, therefore, thought it of interest to compare the binding kinetics of *R*- and *S*-enantiomers of muscarinic antagonists, in order to address the following question: is the receptor stereoselectivity related to different dissociation rate constants, association rate constants, or both?

We chose QNB and methyl-QNB to test this question because (*R*)-QNB and (*R*)-methyl-QNB equilibrate slowly with muscarinic receptors (10–14) and receptor stereoselectivity is not very large (7, 13, 14). We, therefore, hoped that, even if the binding and dissociation kinetics of the low affinity enantiomers [(*S*)-QNB and (*S*)-methyl-QNB] were faster, they would, nevertheless, be slow enough to be measurable. We also suspected that different muscarinic receptor subtypes might have different binding kinetics, and we decided to compare the binding kinetics of the QNB and methyl-QNB enantiomers in homogenates from human NB-OK1 neuroblastoma cells (80% M_1 muscarinic receptors), rat heart (M_2 receptors), and rat pancreas (M_3 receptors) (2, 3).

Validity of the competition kinetics analysis method. We measured the dissociation rate constants of (*R*)-[^{3}H]QNB and (*R*)-[^{3}H]methyl-QNB from NB-OK1 cells and rat heart muscarinic receptors. We did not find any evidence for receptor isomerization in these preparations, with either drug; dissociation rates were constant and independent of the preincubation period used to label the receptors (12) (results not shown). We, therefore, used the "one-step binding" model described by Motulsky and Mahan (8) to analyze competition kinetics. The dissociation rates of (*R*)-methyl-QNB found in competition kinetic experiments were in excellent agreement with the dissociation rates found by direct measurement in NB-OK1 cells and rat heart. The dissociation rates of (*R*)-QNB from rat heart and NB-OK1 muscarinic receptors found by competition kinetics analysis were faster than expected from direct measurement (with the ^{3}H-labeled drug. The differences were, however, not statistically significant. Both tracers labeled a significant population of "nonmuscarinic binding sites" in rat pancreas. We, therefore, did not measure their dissociation rate constants from M_3 receptors in this tissue and limited our measurements to the residual binding to muscarinic sites, 1 hr [with (*R*)-[^{3}H]methyl-QNB] or 4 hr [with (*R*)-[^{3}H]QNB] after atropine addition. Residual (*R*)-[^{3}H]methyl-QNB binding was 37 ± 10%, compared with the 41% expected when using the dissociation rate constant found by competition kinetics. We did not expect,

and did not observe, any (*R*)-[^{3}H]QNB dissociation 4 hr after atropine addition.

We shall hereafter use the constants found by competition kinetics analysis when comparing the rate constants of (*R*)-QNB, (*S*)-QNB, (*R*)-methyl-QNB, and (*S*)-methyl QNB (Table 2).

Comparison of drug binding kinetics to the three muscarinic receptor subtypes. We were surprised previously (3) by the much slower binding kinetics of the nonselective antagonist [^{3}H]NMS to pancreas M_3 receptors, compared with M_1 and M_2 receptors (see Table 1). Our new results suggest that association rate constants of muscarinic antagonists to M_3 receptors might be slow in general; the association rate constants of the *R*- and S-enantiomers of QNB and (*R*)-methyl-QNB (found by competition kinetics) were approximately 10-fold lower at pancreas M_3 receptors than at M_2 or M_1 receptors (Table 2) but were comparable to the association rate of (*R*)-[^{3}H]QNB to pancreatic acini at 37° (5.3×10^5 M^{-1} sec^{-1}; calculated from Ref. 15).

We expected a very slow dissociation rate for (*R*)-QNB from rat pancreas receptors; Larose *et al.* (15) find, at 37°, a half-life of 343 min for (*R*)-[^{3}H]QNB dissociation from rat pancreatic acini, and all reactions are slower at lower temperature (25° in this work). The k_4 value of (*R*)-QNB found by competition kinetics was indeed lower for M_3, as opposed to M_2, receptors (95% confidence interval at M_3 receptors, 0–3.4×10^{-5} sec^{-1}, compared with k_4 from M_2 receptors of 1.5×10^{-4} sec^{-1}). The reaction was, however, too slow to allow us to obtain a valid estimate of either k_4 or K_i for (*R*)-QNB binding to rat pancreas. The dissociation rate constants of (*R*)-QNB and (*R*)-methyl-QNB (found in competition kinetics) varied markedly depending on the receptor subtype (Tables 2 and 3). This was confirmed for M_1 and M_2 receptors with (*R*)-[^{3}H]QNB and (*R*)-[^{3}H]methyl-QNB (see above). (*R*)-QNB (at M_1 and M_2 receptors), (*S*)-QNB, and (*R*)-methyl-QNB (at M_1, M_2, and M_3 receptors), nevertheless, qualified as nonselective drugs because, at equilibrium, their affinities varied <10-fold, when these different receptor subtypes were compared (Table 2). In contrast, (*S*)-methyl-QNB showed a clear preference for M_1 and M_2 over M_3 receptors but similar (rapid) dissociation rates for the three subtypes.

Comparison of binding kinetics of the *R*- and *S*-enantiomers at each muscarinic receptor subtype. As shown in Table 2, the association rate constants of the two enantiomers of either QNB or methyl-QNB were not significantly different. Muscarinic receptor stereoselectivities, which varied between 1- and >60-fold, could be entirely accounted for by variations in dissociation rate constants, with the *S*-enantiomers of QNB and methyl-QNB dissociating faster than the *R*-enantiomers from stereoselective receptors.

These results are compatible with the hypothesis that the association rate constant, reflecting the drug approach into the muscarinic binding site, depends mainly on gross chemical characteristics, such as hydrophobicity, size, presence or absence of a *N*-methyl group, etc. In contrast, the dissociation rate constant measures the breaking of specific, short range interactions between drug and receptor. The dissociation rate constant depends, therefore, on drug stereochemistry to the same extent as equilibrium binding. This is very clear in Table 2, where, for example, (*R*)- and (*S*)-methyl-QNB have the same affinity (same K_i values) and very similar dissociation rate constants for cardiac M_2 receptors but different affinities and dissociation rate constants for pancreas M_3 receptors.

Isomerization of the drug-receptor complex? The association and dissociation kinetics of radiolabeled muscarinic antagonists are often biphasic (10, 11, 16, 17). This was usually interpreted by a two-step reaction mechanism, with two stable forms of drug-receptor complex appearing sequentially during the drug binding reaction (10, 11, 16, 17). We would like to suggest two alternative explanations for this type of result. 1) As previously discussed by Bürgisser *et al.* (18), if the stereoselectivity of the receptor reflects differences in the dissociation rate constant of two enantiomers, biphasic binding kinetics will be observed when a racemic tracer is used. This is due to the rapid binding or dissociation of the low affinity enantiomer, followed by slow binding or dissociation of the high affinity enantiomer. The biphasic binding kinetics observed in rat heart in Ref. 10 (using racemic [^{3}H]QNB) might, therefore, be explained by the different kinetic constants of the two QNB enantiomers (this work). 2) We also demonstrated that different muscarinic receptor subtypes have different association and dissociation rate constants for several nonselective antagonists ([^{3}H]NMS, [^{3}H]QNB, and [^{3}H]methyl-QNB). Because the existence of at least four different receptors has been demonstrated in different brain regions (1, 4), it is quite possible that the biphasic kinetics observed in this tissue with enantiomerically pure or achiral tracers (11, 16) reflect, at least in part, the existence of several receptor subtypes (4–6). In contrast, receptor heterogeneity has not, to our knowledge, been described in chick embryo heart cells; the biphasic antagonist binding kinetics observed in these cells using (*R*)-[^{3}H]QNB (17) might indeed be due to receptor isomerization.

Conclusion. The stereoselectivity of M_1, M_2, and M_3 receptors for binding of QNB and methyl-QNB can be explained by differences in the dissociation rate constants of the *R*- and *S*-enantiomers. The association rate constants of the two enantiomers were not significantly different from each other and were lower in pancreas M_3 receptors than in neuronal M_1 or heart M_2 receptors. The dissociation rate constants of (*R*)-QNB and (*R*)-methyl-QNB (two nonselective antagonists) depended on the receptor subtype.

Acknowledgments

We thank Dr S. Swillens for his nonlinear regression curve-fitting program and M. Stiévenart and N. Peuchot for their excellent secretarial help.

References

1. Bonner, T. I. The molecular basis of muscarinic receptor diversity. *Trends Neurosci.* **12**:148–151 (1989).
2. Waelbroeck, M., J. Camus, M. Tastenoy, and J. Christophe. 80% of muscarinic receptors expressed by the NB-OK1 human neuroblastoma cell line show high affinity for pirenzepine and are comparable to rat hippocampus M1 receptors. *FEBS Lett.* **226**:287–290 (1988).
3. Waelbroeck, M., J. Camus, J. Winand, and J. Christophe. Different antagonist binding properties of rat pancreatic and cardiac muscarinic receptors. *Life Sci.* **41**:2235–2240 (1987).
4. Waelbroeck, M., M. Tastenoy, J. Camus, and J. Christophe. Binding of selective antagonists to four muscarinic receptors (M_1 to M_4) in rat forebrain. *Mol. Pharmacol.* **38**:267–273 (1990).
5. Dörje, F., T. Friebe, R. Tacke, E. Mutschler, and G. Lambrecht. Pharmacological characterization of muscarinic receptors mediating contractions of guinea-pig uterus. *Naunyn-Schmiedeberg's Arch. Pharmacol.* **341**(suppl.):R79 (1990).
6. Waelbroeck, M., M. Gillard, P. Robberecht, and J. Christophe. Muscarinic receptor heterogeneity in rat central nervous system. I. Binding of four selective antagonists to three muscarinic receptor subclasses: a comparison with M_2 cardiac muscarinic receptors of the C type. *Mol. Pharmacol.* **32**:91–99 (1987).
7. Waelbroeck, M., M. Tastenoy, J. Camus, R. Feifel, E. Mutschler, C. Strohmann, R. Tacke, G. Lambrecht, and J. Christophe. Stereoselectivity of the

interaction of muscarinic antagonists with their receptors. *Trends Pharmacol. Sci.* (Suppl. 4) 65–69 (1989).
8. Motulsky, H. J., and L. C. Mahan. The kinetics of competitive radioligand binding predicted by the law of mass action. *Mol. Pharmacol.* **25**:1–9 (1984).
9. Waelbroeck, M., J. Camus, and J. Christophe. Determination of the association and dissociation rate constants of muscarinic antagonists on rat pancreas: rank order of potency varies with time. *Mol. Pharmacol.* **36**:405–411 (1989).
10. Fields, J. Z., W. R. Roeske, E. Morkin, and H. I. Yamamura. Cardiac muscarinic receptors: biochemical identification and characterization. *J. Biol. Chem.* **253**:3251–3258 (1978).
11. Yamamura, H. I., and S. H. Snyder. Muscarinic cholinergic binding in rat brain. *Proc. Natl. Acad. Sci. USA* **71**:1725–1729 (1974).
12. Waelbroeck, M., P. Robberecht, P. Chatelain, and J. Christophe. Rat cardiac muscarinic receptors. I. Effects of guanine nucleotides on high- and low-affinity binding sites. *Mol. Pharmacol.* **21**:581–588 (1982).
13. Lambrecht, G. Cyclische Acetylcholinanaloga. IX. Darstellung und parasympatholytische Wirkung enantiomerer 3-Benziloyloxychinuclidine. *Eur. J. Med. Chem.* **14**:111–114 (1979).
14. Lambrecht, G. Structure and conformation activity relationships of heterocyclic acetylcholine analogues. X. The inhibitory effect of 3-quinuclidinyl benzilates on cardiac mucarinic receptors. *Arzneim. Forsch. Drug Res.* **12**:2113–2115 (1980).
15. Larose, L., Y. Dumont, J. Asselin, J. Morisset, and G. G. Poirier. Muscarinic receptor of rat pancreatic acini: [^{3}H]QNB binding and amylase secretion. *Eur. J. Pharmacol.* **76**:247–254 (1981).
16. Kloog, Y., Y. Egozi, and M. Sokolovsky. Characterization of muscarinic acetylcholine receptors from mouse brain: evidence for regional heterogeneity and isomerization. *Mol. Pharmacol.* **15**:545–558 (1979).
17. Galper, J. B., L. C. Dziekan, D. S. O'Hara, and T. W. Smith. The biphasic response of muscarinic cholinergic receptors in cultured heart cells to agonists. *J. Biol. Chem.* **257**:10344–10356 (1982).
18. Bürgisser, E., R. J. Lefkowitz, and A. De Lean. Alternative explanation for the apparent "two step" binding kinetics of high-affinity racemic antagonist radioligands. *Mol. Pharmacol.* **19**:509–512 (1981).

Send reprint requests to: Jean Christophe, Department of Biochemistry and Nutrition, Medical School, Université Libre de Bruxelles, Boulevard of Waterloo 115, B-1000 Brussels, Belgium.